CO12-1

Development of a non-destructive assay technique for nuclear material detection and U enrichment measurement by photonuclear reaction induced by bremsstrahlung X-ray
(1) Grand plan

H. Sagara[1], K. Tanabe[2], T. Katabuchi[1], K. Terada[3], Y. Takahashi[3], J. Hori[3]

[1] *Institute of Science Tokyo*
[2] *National Research Institute of Police Science*
[3] *Institute for Integrated Radiation and Nuclear Science, Kyoto University*

Development of a non-destructive assay technique for nuclear material detection and U enrichment measurement by photonuclear reaction has been conducted induced by external high-energy photon source. In the present research, focusing on the bremsstrahlung X-ray source technically established and available, the following 4 items are planned to be conducted; (1) development of nuclear material detection method, (2) development of its detector system, (3) demonstration experiment, and (4) nuclear data evaluation, and the research goal is to verify the principles of non-destructive assay technique for nuclear material detection and U enrichment measurement. Montecarlo simulation results of Bremsstrahlung X-ray spectrum and Photo-fission cross-section of ^{235}U, ^{238}U are shown in Fig. 1[1]. With combination of the initial energy of accelerated electron, different response from uranium is expected according to the energy dependence of photo-fission reaction cross-section and uranium isotopes, the correlation of uranium enrichment to the reaction response is expected and the demonstration experiments have just begun in 2025[1-2].

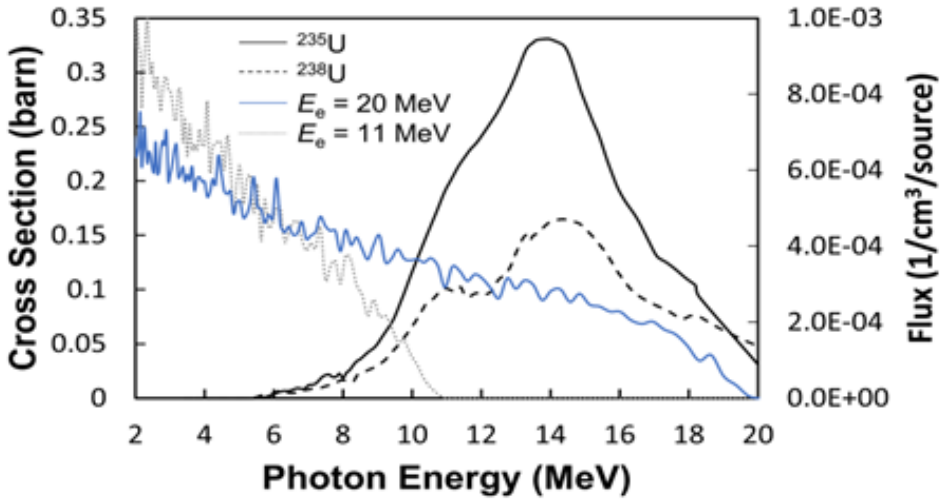

Fig. 1. Photo-fission cross-section of ^{235}U, ^{238}U and Bremsstrahlung X-ray spectrum [1]

REFERENCES:

[1] H. SAGARA *et al.,* Pro-ceedings, 46th Annual Meeting of Institute of Nuclear Material Management Japan Chapter, #4604, 2025.
[2] K. Kiatkongkaew *et al.,* Pro-ceedings, 46th Annual Meeting of Institute of Nuclear Material Management Japan Chapter, P4656, 2025.

CO12-2

Homogeneity of radioactivity in the stainless steel sample produced by nuclear reactor neutron irradiation

T. Miura[1], K. Takamiya [2]

[1] *National Institute of Advanced Industrial Science and Technology*
[2] *Institute for Integrated Radiation and Nuclear Science, Kyoto University*

INTRODUCTION: The ongoing decommissioning project at the Tokyo Electric Power Company's Fukushima Daiichi Nuclear Power Station requires the measurement of radioactivity in large quantities of samples, including debris, metal, and sludge [1]. Ensuring the validity and reliability of these radioactivity measurements is an essential requirement for the implementation of this decommissioning project, which is the subject of significant public interest. To ensure validity and reliability, it is effective to verify the validity of the operator's measurements using test samples that contain a uniform concentration of the target nuclide and for which the radioactivity per unit mass has been calibrated. In this study, as a preliminary experiment for the preparation of metallic test specimens, we verified the homogeneity of radionuclides produced by irradiating stainless steel reference materials in a nuclear reactor.

EXPERIMENTS: Japanese Iron and Steel certified reference material JSS 652-17 (stainless steel 316) was used for neutron irradiation sample. The certified values in JSS 652-17 are Mn (0.961 ± 0.004) %, Cr (16.8 ± 0.04) %, and Mo (2.04 ± 0.01) %, respectively. Five samples of approximately 10 mg of JSS 652-17 were weighed using a METTLER TOLEDE XP26V micro balance and heat-sealed in the polyethylene bags. The samples were irradiated for 5 min using KUR PN2 (neutron fluence rate: 5×10^{12} n $cm^{-2}s^{-1}$). After cooling for 1 day, the produced ^{51}Cr, ^{56}Mn, and ^{99}Mo in the sample were measured using Ge detector (ORTEC GEM25185).

RESULTS: The decay corrected measured values at the end of the irradiation are shown in Table 1. Analysis of variance of the measured values revealed that only ^{51}Cr showed statistically significant differences between samples. These results indicate that it is difficult to produce homogeneous samples solely through neutron activation by simple pneumatic irradiation facility.

Table 1 Measured results radioactive nuclides in the JSS 652-27 (stainless steel 316)

Sample No.	Measured No.	^{51}Cr cps/mg	^{56}Mn cps/mg	^{99}Mo cps/mg
No. 1	1st	1.20 ± 0.53 %	1405 ± 0.24 %	1.80 ± 0.51 %
	2nd.	1.23 ± 0.42 %	1453 ± 3.7 %	1.99 ± 0.45 %
No.2	1st	1.25 ± 0.73 %	1474 ± 0.37 %	1.90 ± 0.71 %
	2nd.	1.30 ± 0.43 %	1605 ± 4.3 %	2.09 ± 0.43 %
No.3	1st	1.29 ± 0.91 %	1498 ± 0.91 %	1.99 ± 0.92 %
	2nd.	1.30 ± 0.54 %	1636 ± 7.2 %	2.15 ± 0.56 %
No.4	1st	1.28 ± 0.90 %	1495 ± 0.70 %	2.01 ± 0.84 %
	2nd.	1.32 ± 0.65 %	1555 ± 0.64 %	2.09 ± 0.67 %
No.5	1st	1.34 ± 0.92 %	1543 ± 0.65 %	2.08 ± 0.87 %
	2nd.	1.34 ± 0.49 %	1548 ± 0.56 %	2.12 ± 0.45 %
Mean ± RSD%		1.29 ± 3.5 %	1520 ± 4.6 %	1.29 ± 3.5 %

Each value after "±" indicates the counting statistics.

REFERENCE:

[1] https://www.dd.ndf.go.jp/files/user/pdf/en/strategic-plan/book/20251225_SP2025eFT.pdf

CO12-3

Study on the Calibration Method for ^{41}Ar Using an Inner-Through Type Ionization Chamber with a Commercial Gas Monitor

R. Furukawa[1], T. Yamada[2,4], H. Yashima[3], Y. Soeta[4] and K. Nakahara[5]

[1]*National Metrology Institute of Japan, Advanced Industrial Science and Technology*
[2]*Atomic Energy Research Institute, Kindai University*
[3]*Institute for Integrated Radiation and Nuclear Science, Kyoto University*
[4]*Graduate School of Science and Engineering Research, Kindai University*
[5]*Faculty of Science and Engineering Research, Kindai University*

INTRODUCTION: In order to calibrate gas monitors used for measuring radioactive noble gases in nuclear facilities, use of activity reference measurement standard gases shall be required. ^{41}Ar is one of potentially released noble gas from nuclear facilities. And the primary concentration standard for ^{41}Ar, is currently under development at the National Metrology Institute of Japan (NMIJ). In previous study, the response of an inner-through type Ionization Chamber (IC) was calibrated using the activity concentration of ^{41}Ar determined by absolute measurement with the proportional counters [1]. In the preceding fiscal year, the authors measured ^{41}Ar using the IC and evaluated the response ratio of them between P-10 gas (Ar: 90 %, CH4: 10 %), used in proportional counter measurements, and dry air [2]. Based on this result, we successfully determined ^{41}Ar concentration using the IC when air was employed as the ionization medium. In the present study, with the aim of establishing a calibration system for ^{41}Ar, calibration method using the IC was examined with a commercially available ionization-chamber-type gas monitor.

EXPERIMENTS: Acrylic container (≈3 ml) was filled with Pure Argon gas. And ^{41}Ar gas was produced via ^{40}Ar(n, γ)^{41}Ar reaction. Samples were irradiated for 60 s at the bottom of KUR-SLY under operating at 1 MW thermal output. The gamma-ray spectrum of an irradiated ^{40}Ar sample measured using a High-Purity Ge (HPGe) semiconductor detector, the production of ^{41}Ar was confirmed without any impurities. As a test case for calibration, the AlphaGUARD (Bertin Technologies SAS)—an ionization-chamber-based commercial radon monitor—was employed. A gas loop including the IC and the AlphaGUARD was constructed. After sufficient evacuation, ^{41}Ar was injected from the acrylic container into the gas loop, and dry air was subsequently added up to approximately one atmosphere. The gas mixture was then circulated for about 15 minutes using a circulation pump to ensure homogeneity.

RESULTS: On the order of several tens of pA was measured with the IC, which corresponds to an ^{41}Ar concentration of approximately 200 Bq cm^{-3}. An increase in the output of the AlphaGUARD was also observed after the injection of ^{41}Ar, indicating the feasibility of calibrating gas monitors using the IC employed in this study. However, because the AlphaGUARD provides output in terms of radon concentration by default, and problems such as the gas tightness, the evaluation of a calibration factor was not achieved. In future work, the system will be improved, and experiments using other gas monitors will be considered, with the aim of developing a robust and reliable calibration method.

REFERENCES:

[1] A. Yunoki *et al.*, KURNS Progress Report 2019 (2020) CO12-5, 275
[2] R. Furukawa *et al.,* Appl. Radiat. Isot. **226** (2025) 112211

CO12-4

Performance Evaluation of Prompt Response with Cobalt Emitter SPND

T. Azuma[1], M. Sasano[1], R. Tanaka[2], M. Hayashi[1], Y. Yoshino[3] and C. H. Pyeon[3]

[1] *Advanced technology R&D center, Mitsubishi Electric Corporation*
[2] *Energy systems center, Mitsubishi Electric Corporation*
[3] *Institute for Integrated Radiation and Nuclear Science, Kyoto University*

INTRODUCTION: For the safety and autonomous control of next-generation reactors such as Small Modular Reactors (SMRs), in-core neutron flux monitoring with high time resolution is essential. Self-powered neutron detectors (SPNDs) are widely employed for this purpose due to their durability in high-radiation environments. In our previous studies, we evaluated the feasibility of rhodium (Rh) and vanadium (V) emitter SPNDs. While the "delayed-type" emitters of Rh and V provide high sensitivity, they require digital compensation to correct for time delays caused by the half-life of beta decay (e.g., 3.74 min for ^{52}V). In this study, we evaluated a Cobalt (Co) emitter SPND, which is categorized as a "prompt-type" detector [1], to verify its instantaneous response during rapid reactor power changes.

EXPERIMENTS: Measurement was performed at the Kyoto University Reactor (KUR) using the Slant exposure tube (SLANT). The reactor power was varied between 1 and 5 MW to assess the dynamic response of the Co-SPND. The current output was measured using a high-precision digital measurement device [2]. In contrast to Rh and V emitters, which rely on beta decay, the Co emitter generates a signal primarily through prompt γ-ray emission and subsequent internal conversion or photoelectric effects following neutron capture via the ^{59}Co (n, γ) ^{60}Co reaction.

RESULTS: Figure 1 shows the Co-SPND output current during the reactor thermal power ramp-up. Compared to the V-SPND [3], which requires physical model-based deconvolution due to significant response delays, the raw output of the Co-SPND tracked the reactor power increase near-instantaneously. Although Co-SPNDs accumulate a long-term background signal from ^{60}Co ($T_{1/2}$ = 5.26 years), it was confirmed that the prompt component dominates the signal during transient operations, providing sufficient accuracy for real-time monitoring without complex deconvolution. The characteristics underscore the suitability of Co-SPNDs for safety protection systems requiring rapid response to power excursions. However, it was observed that the output current began to decrease immediately after the reactor reached the 5 MW plateau. The current eventually dropped to approximately 60% of the expected value based on the initial sensitivity. Further investigations are planned to clarify the underlying physical mechanism of this phenomenon to ensure the reliability and accuracy of Co-SPNDs for steady-state monitoring at rated power.

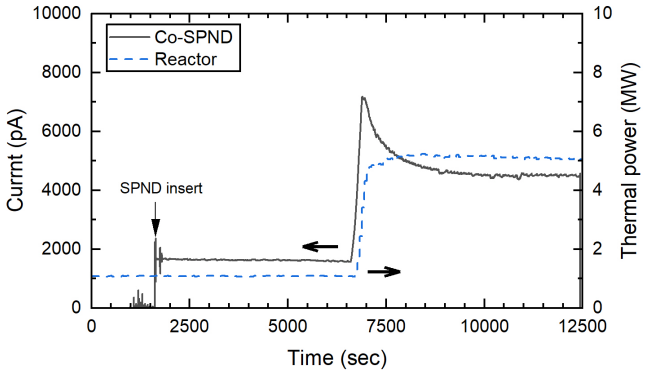

Fig. 1. Time trend of measured signal current to reactor power variation at SLANT.

REFERENCES:

[1] N. P. Goldstein and W. H. Todt, IEEE Trans. Nucl. Sci., **NS-26** (1979) 916-923.
[2] R. Tanaka *et al.*, Mitsubishi Electric ADVANCE, September 2025 (2025) 14.
[3] M. Sasano *et al.*, KURNS Progress Report 2024 (2025) 251.

CO12-5

Experimental Study on Fission Chamber Response in High Neutron Flux at KUR Heavy Water Neutron Irradiation Facility

T. Azuma[1], M. Sasano[1], R. Tanaka[2], M. Hayashi[1], H. Tanaka[3] and C. H. Pyeon[3]

[1] *Advanced technology R&D center, Mitsubishi Electric Corporation*
[2] *Energy systems center, Mitsubishi Electric Corporation*
[3] *Institute for Integrated Radiation and Nuclear Science, Kyoto University*

INTRODUCTION: Accurate monitoring of neutron flux, from reactor startup to full-power operation, is critical for the safety and control of next-generation reactors. Fission chambers (FCs) coated with uranium-235 are primary instruments for this purpose; however, they must transit between the pulse mode and Campbelling modes to cover a wide dynamic range. A seamless transition in the "overlap region" is essential for continuous monitoring, yet it requires rigorous verification under high-flux irradiation to account for pulse pile-up effects. The study was conducted at the Heavy Water Neutron Irradiation Facility of the Kyoto University Reactor (KUR-HWNIF) to evaluate FC performance under high-count-rate conditions.

EXPERIMENTS: Experiments were carried out at KUR-HWNIF, operating at a constant reactor power of 5 MW. The high-power operation is essential for achieving a maximum neutron flux of approximately 1×10^{9} $cm^{-2}\cdot s^{-1}$ [1], enabling performance evaluation under high-count-rate conditions. To evaluate the detector response across varying intensities, the thermal neutron flux was adjusted by varying the distance from the irradiation port and the thickness of polyethylene (PE) moderators, as summarized in Table 1. The primary objective of experiments was to validate the detector response within the Campbelling mode regime using the signal processing unit [2], specifically targeting the high-output range above 1×10^{8} $s^{-1}\cdot cm^{-2}$. Additionally, measurements were performed in the overlap region to verify the seamless transition between the pulse and Campbelling modes.

RESULTS: As shown in Figure 1, the experiments at KUR-HWNIF demonstrated linear detector responses across a thermal neutron flux of 4.1×10^{6} to 1.5×10^{8} $cm^{-2}\cdot s^{-1}$. Linearity in pulse mode was confirmed from 2.9×10^{5} to 8.2×10^{5} cps, while the Campbelling mode (equivalent count rate) covered 3.1×10^{5} to 6.6×10^{6} cps. An overlap region of more than one order of magnitude was successfully established between the two measurement modes. Furthermore, by applying dead-time corrections to account for pulse pileup, the overlap was expected to extend to approximately two orders of magnitude. The findings validated the system's capability for seamless, wide-range neutron monitoring and demonstrated the high reliability of the FC under high-count-rate conditions.

Table 1. Irradiation conditions and corresponding thermal neutron flux.

PE thickness [mm]	Distance [mm]
without	0
without	240
40	240
100	240

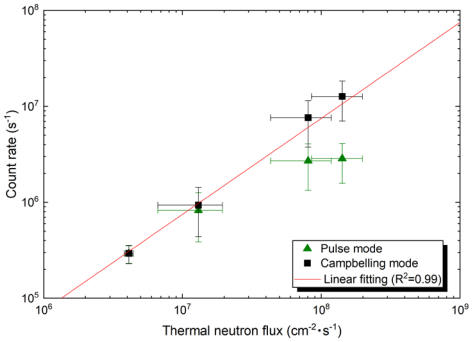

Fig. 1. Linearity of neutron flux to count rate at KUR-HWNIF.

REFERENCES:

[1] Y. Sakurai *et al.*, Nucl. Instr. and Meth., **453** (2000) 569-596.
[2] R. Tanaka *et al.*, Mitsubishi Electric ADVANCE, September 2025 (2025) 14.

CO12-6

A texture analysis of the excavated early medieval *Haji*-ware of different colour by INAA

M. Tomii[1], K. Takamiya[2], M. Inagaki[2], A. Ito[3], M. Kidachi[4], and T. Tateishi[5]

[1] *Faculty of Literature, Taisho University*
[2] *Institute for Integrated Radiation and Nuclear Science, Kyoto University*
[3] *Graduate School of Letters, Kyoto University*
[4] *College of Letters, Ritsumeikan University*
[5] *Agency for Cultural Affairs*

INTRODUCTION: To investigate the reason for the colour difference –white/red– of the early medieval low-temperature-fired pottery (*Haji*-ware), a collection of large number of *Haji*-ware of 13th century, excavated from a rather deep and large deposition in the campus of Kyoto University [1], is examined. It is mainly composed of the classic six types of the early medieval Kyoto *Haji-ware*: white larger bowl, white small bowl, white coaster-shaped plate, reddish medium-sized plate, reddish small plate, and reddish coaster-shaped plate. The four major types, excluding white/reddish coaster-shaped ones, are analyzed this year.

EXPERIMENTS: Conventional INAA was applied to determine the elemental composition of samples of the *Haji*-ware, each of whose main body had been drilled, or scraped, by the alumina [Al2O3] drill into fine powder as a sample after removing off the very surface, and then had been enclosed in a polyethylene bag [2]. Every of above-mentioned four types of the *Haji*-ware has seven samples respectively from different pieces. Each of the 28 samples was neutron-irradiated at Pn-3 (1 MW for 90 seconds) for short-lived nuclides, and at Pn-2 (5 MW for 1 hour) for long-lived ones. The gamma-ray spectrometry of the irradiated samples was performed after the irradiation, and the k_0-standardization method for determination of concentration of elements was performed. For the k_0 method, three standard elements, Au, Lu and Zr, were prepared as a comparator.

RESULTS: With irradiation by Pn-3, concentrations of eleven elements (As, Eu, Ga, K, La, Mg, Mn, Na, Sm, Ti, and V) in almost every 28 sample were determined. The determination for samples irradiated by Pn-2 has not completed so far. From the short-lived nuclides two results can be pointed out here; (i) Na and Mn show clear difference in concentration to divide 28 samples into two groups, which fully correspond with the colour groups (Figs.1&2), and (ii) La cannot be the marker of colour difference, which was for the 14th century *Haji*-ware (Fig. 1). These results may suggest that the colour difference was brought by the texture difference, and that the preparation for clay texture to form the body of ware in 13th century differed from that in 14th century.

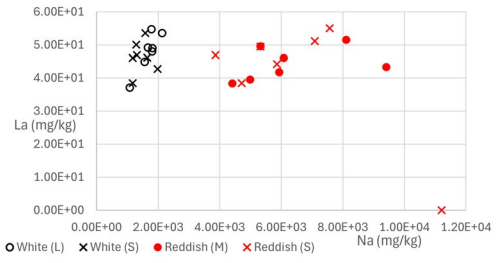

Fig.1 Distribution of 28 samples on the concentrations combination of Na with La.

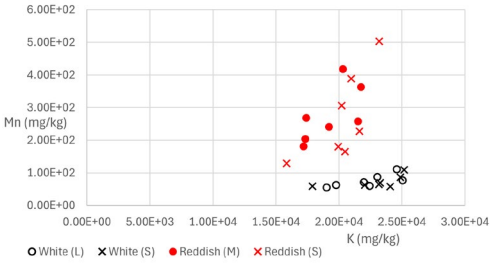

Fig.2 Distribution of 28 samples on the concentrations combination of Mn with K.

REFERENCES:

[1] A. Ito 'Large rubbish pit beside the Shirakawa-road', Y. Chiba (ed.) *Reconstruction of Historical Image of the Suburbs of Kyoto City Based on Research on Shirakawa-road.* (2012) 103-128.
[2] J. Sterba, *J. Radio. Nucl. Chem.*, **316** (2018) 753-759

CO12-7

Development of Radiation Monitor for Space weather measuring Electrons (RMS-e) and Protons (RMS-p) for the Himawari-10 satellite

T. Namekawa[1], K. Otsuji[1], I. Park[1], S. Saito[1]

[1] *National Institute of Information and Communications Technology*

INTRODUCTION: Monitoring of the radiation environment in geostationary orbit around the Earth is very important for space weather forecast. However, the instruments on board the Himawari 8 and 9 meteorological satellites, which are currently operating, have an insufficient energy range and energy resolution to fully monitor the space radiation environment. Therefore, we are developing the Radiation Monitor for Space Weather measuring Electrons (RMS-e) and the Radiation Monitor for Space Weather measuring Protons (RMS-p) instruments for installation on the next Himawari meteorological satellite. The RMS-e instrument is designed to measure the energy and flux of electrons between 50 keV and 6 MeV, while the RMS-p instrument is designed to measure the energy and flux of protons between 10 and 500 MeV, using stacked solid-state detectors (SSDs) made of silicon semiconductors. We evaluated the measurement range for electron energy and the energy resolution of > 2 MeV electrons by irradiating electrons emitted by the Kyoto University Institute for Integrated Radiation and Nuclear Science Linear Accelerator (KURNS-LINAC) onto the engineering model (EM) of the RMS-e instrument. We also evaluated the degree to which electron contamination could contribute to noise in proton observations by irradiating electrons emitted by the KURNS-LINAC to the RMS-p EM.

EXPERIMENTS: RMS-e EM and RMS-p EM were installed in the irradiation room and the monoenergetic electron beam generated by LINAC was injected. The electron energies injected into RMS-e EM were 2.2, 2.6, 2.95, 3.3, 3.9, 4.5, 5.25, 6, and 7 MeV perpendicular to the stacked SSDs. The electron energies injected into RMS-p EM were 2.2, 10, and 30 MeV perpendicular to the stacked SSDs, and perpendicular to the plastic scintillator for eliminating oblique incidence. The outer circumference of the instruments was covered with lead blocks for radiation protection.

RESULTS: Figure 1 shows the energy spectrum obtained using RMS-e EM for all incident electron beams (2.2, 2.6, 2.95, 3.3, 3.9, 4.5, 5.25, 6, and 7 MeV). The energy resolution based on the full width half maximum of the peaks is about 10% for electrons below 5 MeV. Considering the losses caused by electron scattering from the Al shield installed at the entrance and the penetration of high-energy electrons, as well as the small number of detected electrons at very low beam flux, these energy resolutions are sufficient to monitor the high-energy electrons in geostationary orbit around the Earth.

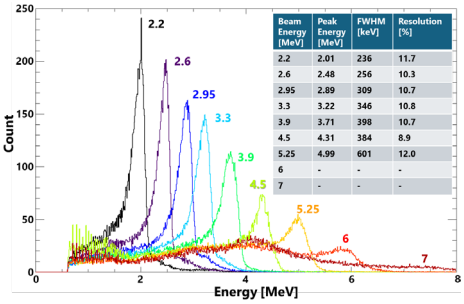

Beam Energy [MeV]	Peak Energy [MeV]	FWHM [keV]	Resolution [%]
2.2	2.01	236	11.7
2.6	2.48	256	10.3
2.95	2.89	309	10.7
3.3	3.22	346	10.8
3.9	3.71	398	10.7
4.5	4.31	384	8.9
5.25	4.99	601	12.0
6	-	-	-
7	-	-	-

Figure 1. The electron energy spectra measured by RMS-e EM (2.2, 2.6, 2.95, 3.3, 3.9, 4.5, 5.25, 6 and 7 MeV).

Figure 2 shows the result obtained using RMS-p EM for all incident electron beams (2.2, 10, and 30 MeV). A portion of the >10 MeV electrons become contamination when irradiated onto a stacked SSDs, and >30 MeV electrons become contamination when irradiated onto the scintillator. Considering the prevalence of these electrons in orbit, they have virtually no effect on proton observations.

These results confirm that the performance of these instruments is sufficient for measuring the radiation environment in geostationary orbit.

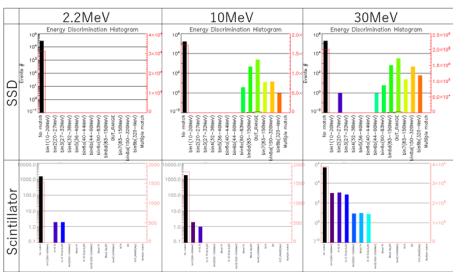

Figure 2. The electron energy discrimination by RMS-p EM (2.2, 10 MeV and 30 MeV).

CO12-8

Observation of Internal Pore Distribution in Additively Manufactured Metal Fabricated by Electron Beam Powder Bed Fusion

Y. Seki[1], T. Chiba[2], K. Wako[2], and M. Hino[3]

[1] *Institute of Multidisciplinary Research for Advanced Materials, Tohoku University*
[2] *New Industry Creation Hatchery Center, Tohoku University*
[3] *Institute for Integrated Radiation and Nuclear Science, Kyoto University*

INTRODUCTION: Metal additive manufacturing is widely regarded as a powerful fabrication approach, enabling the fabrication of complex geometries that are difficult to achieve with conventional methods and contributing to weight reduction and functional optimization. However, the process inherently involves rapid melting and solidification and therefore tends to generate internal defects such as microscopic pores. These features can influence the mechanical and functional performance of the final component.

In general, porosity in metal additively manufactured products has been evaluated through destructive techniques, including cross-sectional analysis with optical microscopy. Although such methods provide detailed local information, they are not suitable for evaluating the internal structure of an entire component without damage. To overcome this limitation, we are developing a non-destructive technique based on neutron phase imaging at the CN-3 port of KUR to visualize the porosity distribution within additively manufactured metal structures [1]. By employing a grating interferometer to detect small-angle neutron scattering caused by micropores, it becomes possible to probe the interior of relatively thick samples. This approach also enables observation over a wide area on the order of several tens of square centimeters.

EXPERIMENTS: The samples were approximately 1 cm^3 cubes of INCONEL 718 fabricated by electron beam powder bed fusion under different process parameters. Pores with diameters ranging from sub-micrometer to micrometer scales induce small-angle neutron scattering. In this measurement, the "correlation length" [2, 3] of the scattering imaging was set to 0.5 μm. The total exposure time was 640 s under a reactor thermal power of 5 MW.

RESULTS: Figure 1(a) shows the scattering image obtained by neutron phase imaging. In this image, darker regions correspond to areas where small-angle neutron scattering is more pronounced, indicating the presence of a larger amount of microporosity within the material. Fig. 1(b) plots the visibility reduction averaged over the entire sample against the average relative density evaluated by the Archimedes method. A correlation between the neutron scattering contrast and the bulk density is observed. Further comparison with X-ray CT is planned for future work.

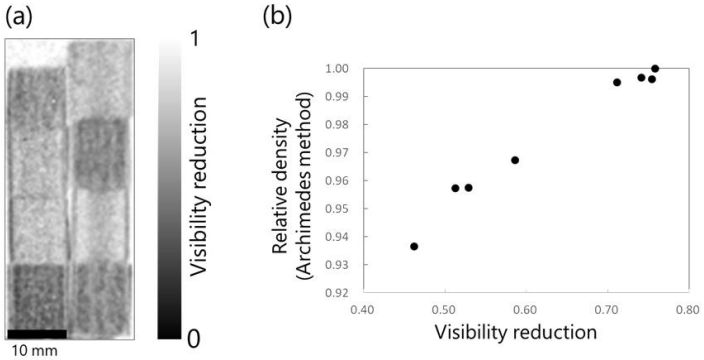

Fig. 1. (a) Neutron scattering image of the additively manufactured metal samples. (b) Correlation between the visibility reduction and the relative density evaluated by the Archimedes method.

REFERENCES:

[1] Y. Seki et al., Rev. Sci. Instrum., 94, 103701 (2023).
[2] W. Yashiro et al., Opt. Exp 18, 16890 (2010).
[3] M.Strobl et al., Sci. Rep. 4, 7243 (2014).

CO12-9

Testing of a Neutron Scintillation Detector at KUR CN-3

H. Ohshita[1], S. Matoba[1], S. Kanda[1], H. Endo[1], T. Seya[1] and M. Hino[2]

[1] *Institute of Materials Structure Science, KEK*
[2] *Institute of Integrated Radiation and Nuclear Science, Kyoto University*

INTRODUCTION: A flat-panel resistor-type photomultiplier (FRP) detector is a simple two-dimensional neutron detector. ^{6}LiF/ZnS(Ag) and ^{6}Li glass scintillators are widely used for neutron detection. The two scintillators can be purchased from Scintacor Co. Ltd. under the trade names ND Screen (ND) and GS20, respectively. GS20 outperforms ND in terms of the expected neutron efficiency and rate characteristics of the generated signal, whereas ND produces a much greater light yield. Furthermore, ND offers a cost advantage when scaled to large active areas. ND has a better positional resolution than GS20. This is because the transparent GS20 allows scintillation light from various angles of incidence to enter the photomultiplier, thereby increasing the light spread. Thus, because ND and GS20 have distinct advantages and disadvantages, they must be selected based on specific applications. In this paper, we report the results of neutron irradiation tests conducted at KUR CN-3 using GS20 (FRP-GS20) as the neutron scintillation detector.

EXPERIMENTAL RESULTS: In neutron irradiation tests using FRP-GS20, the detector was installed downstream of the disc chopper in CN-3, and the neutron efficiency and position resolution were measured using the neutron time-of-flight method. The experimental setup and measurement methods were almost identical to those used in our previous studies. The neutron intensity of CN-3 was derived to measure the neutron efficiency, as shown in Figure 1. This result was obtained using a neutron detector filled with ^{3}He gas. The neutron beam was collimated to 1 cm × 1 cm using a B_4C resin collimator, and its wavelength dependence was calculated from the time of flight relative to the opening time of the disk chopper. The peak value of the CN-3 neutron intensity was 1.9 Å, and the neutron flux was 651 neutrons/s·cm^2. Figure 2 shows the measured neutron efficiency of FRP-GS20. These results were derived as the FRP-GS20 count values corresponding to the neutron intensities of CN-3 in the 1–6 Å range. The thermal neutron efficiency was 66%, which was slightly lower than that provided by the manufacturer. This was attributed to the low nγ discrimination capability in the pulse height distribution, resulting in a failure to count all neutron components. Figure 3 shows a two-dimensional image of a multi-pinhole array (pinhole diameter: 1 mm, pinhole pitch: 5 mm) fabricated from a Cd plate. The pinhole pitch was distorted at the edges owing to the use of a resistive chain readout. Based on this result, the two-dimensional image from the FRP-GS20 was corrected to absolute values, and the expected spatial resolution was 1.4 mm (full width at half maximum). This value was lower than that obtained using ND, attributed to the characteristics of the scintillator, as mentioned earlier. In the future, to improve the spatial resolution, we plan to reoptimize the configuration of FRP-GS20 and perform simulations using Geant4 to evaluate the validity of the measurement data.

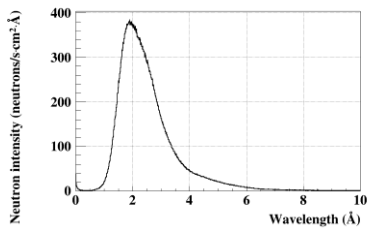

Figure 1. Neutron intensity of CN-3

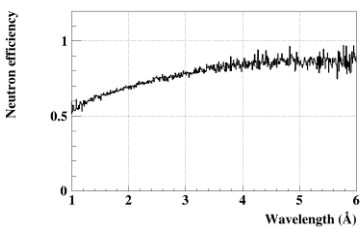

Figure 2. Neutron efficiency of FRP-GS20

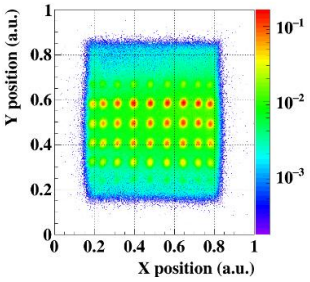

Figure 3.
2D multi-pinhole image

CO12-10

Study of Isotope Separation via Chemical Exchange Reaction

R. Hazama[1], P. Kumsut[1], T. Yoshimoto[1], A. Rittirong[2], C. Pitakchaianan[1], K. Kosinarkaranun[1], Y. Sakuma[3], T. Fujii[4], T. Fukutani[5], Y. Shibahara[5], and T. Kishimoto[2]

[1]*Graduate School of Human Environment, Osaka Sangyo University*
[2]*Research Center for Nuclear Physics, Osaka University*
[3]*Laboratory for Zero-Carbon Energy, Institute of Science Tokyo*
[4]*Graduate School of Engineering, Osaka University*
[5]*Institute for Integrated Radiation and Nuclear Science, Kyoto University*

INTRODUCTION: Chemical isotope separation for calcium and lithium has been studied by liquid-liquid extraction (LLE) with DC18C6 crown-ether [1]. This report describes the distribution coefficient and the isotope separation factor under the various reaction temperatures.

EXPERIMENTS: The experiment was carried out at –15, 0, room temperature (22±0.5), and 45 °C reaction temperature. 30% w/w $CaCl_2$/LiCl (aqueous solution) and 0.07M DC18C6 dissolved in chloroform, with a volume ratio of 1/10, as an aqueous and organic phase were mixed in the incubator with a several temperatures for 1 hour. The extraction process was conducted at room temperature for 1 minute and allowed for phase separation in the separation funnel for 10 minutes under the constant room temperature condition [1].

RESULTS: The results of temperature dependency indicated that the distribution coefficient (D) increases as the temperature decrease. The same behavior was observed on both calcium and lithium extraction. This finding was in good agreement with K. Nishizawa et al. report on the study of lithium extraction using crown-ether and temperature difference, ranging from 0 ~ 40 °C [2]. The results revealed the same behavior as our finding. However, K. Nishizawa carried out the extraction by 2M LiI, was the most applicable species due to the high distribution coefficient (D) and a high concentration of B15C5 (0.186M) under the same volume of organic and aqueous phase (20mL/20mL). The results indicated the dependency on separation factor (α) up to 1.045 at 0 °C.

Reaction Temperature ℃	$CaCl_2$ (aq) (M)	Distribution Coefficient (D)	The mole ratio between ion-crown complex to the total crown-ether	$^{48}Ca/^{40}Ca$ Separation factor (α_{org})
–15	3.6	3.4×10^{-2}	0.16	0.987±0.003
0	3.6	3.0×10^{-2}	0.14	0.989±0.005
22	3.7	2.3×10^{-2}	0.12	0.990±0.003
45	3.6	1.6×10^{-2}	0.074	0.990±0.003

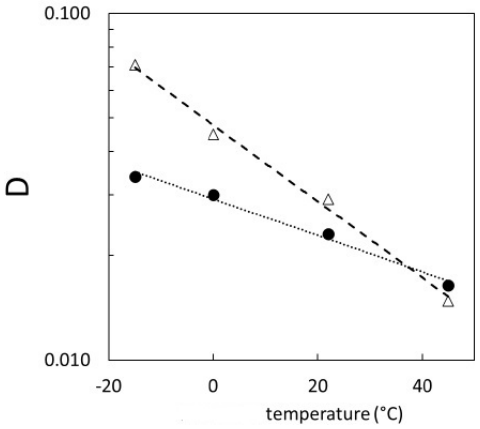

Fig. 1. The distribution coefficient (D) of calcium and lithium extraction on various reaction temperature (℃). Filled circle for Ca and open triangle for Li, respectively.

REFERENCES:

[1] A. Rittirong, Doctor Thesis, OSU (2022).
[2]K. Nishizawa et al, J. Nucl. Sci. Tec.21,694(1984).

CO12-11

Encapsulation of Lubricant Additives - Enhanced Lubrication Performance through Micellar Solubilization of Poorly Soluble Additives by Surfactants

T. Hirayama[1], H. Gu[1], N. Yamashita[2] and M. Hino[3]

[1] *Department of Mechanical Engineering and Science, Graduate School of Engineering, Kyoto University*
[2] *Department of Mechanical and System Engineering, Kyoto Institute of Technology*
[3] *Institute for Integrated Radiation and Nuclear Science, Kyoto University*

INTRODUCTION: In industrial machinery, lubrication is essential for reducing friction and wear and improving efficiency; however, conventional mineral oil-based lubricants pose challenges such as flammability and environmental pollution. As an alternative, water-based lubricants offer superior safety and environmental compatibility, but they require improvement due to issues with lubrication performance and corrosion. While additives such as nanoparticles and ionic liquids have been studied, challenges remain regarding dispersion and cost. On the other hand, organic additives are environmentally friendly and offer high lubrication performance, but they have the drawback of being poorly soluble in water. To address this issue, this study proposes a new method that utilizes micellization to encapsulate organic additives and disperse them uniformly in water.

SAMPLES: Aqueous solution with a 2HDNa concentration of 100 mM was prepared by neutralization reaction of 2-hexyldecanoate (>98%, Tokyo Chemical Industry) with NaOH (>97%, FUJIFILM Wako Pure Chemical Corporation). Our previous research demonstrated that the critical micelle concentration (CMC) of 2HDNa is approximately 25 mM [16]. Therefore, we chose a concentration of 100 mM. In addition, palmitic acid (>95 %, FUJIFILM Wako Pure Chemical Corporation) was selected as a model additive.

EXPERIMENTS AND RESULTS: FTIR spectroscopy and SAXS confirmed the successful solubilization of C16 within 2HDNa micelles, preserving its original molecular structure. Tribological experiments demonstrated that the addition of C16 significantly reduced the coefficient of friction, achieving a maximum reduction of over 33%. QCM-D and NR analyses were used to evaluate the adsorption performance. A lubrication mechanism was proposed in which micelles deform under external pressure, releasing the encapsulated C16, which then forms an effective boundary lubrication layer. These findings highlight micellar solubilization as a promising and efficient strategy for enhancing the performance of water-based lubricants.

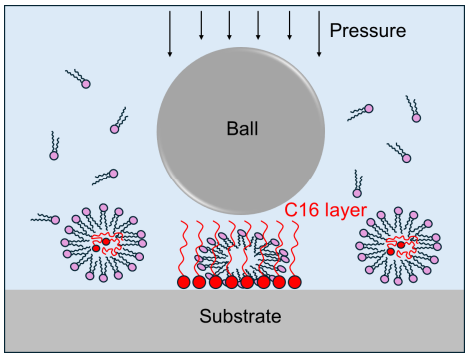

Fig. 1. Schematic illustration of the proposed lubrication mechanism by Micellar Solubilization.

REFERENCES:

[1] H. Gu, T. Hirayama, N. Yamashita, T. Okano, J. Xu, N. Sato et al., Tribological performance of a surfactant derived from its structure of molecular aggregates in water, Tribology International, 188 (2023) 108881.

CO12-12

Neutron shielding performance of novel lead-free iron oxide ceramics

H. Terato[1], and Y. Sakurai[2]

[1]*Advanced Science Research Center, Okayama University*
[2]*Institute for Integrated Radiation and Nuclear Science, Kyoto University*

INTRODUCTION: Shielding is a critical safety procedure in the handling of ionizing radiation. When selecting shielding materials, it is necessary to consider appropriate options based on the type and energy of the radiation. For the shielding of γ-rays and X-rays, which are most frequently encountered, lead blocks are commonly employed. However, there is a global trend toward phasing out lead due to its inherent toxicity [1]. We have previously evaluated the γ-ray shielding performance of a novel lead-free iron-oxide-based ceramic to explore its potential as a substitute material [2]. Our prior results demonstrated its efficacy as a shielding material against γ- and X-ray radiation. To further investigate whether this novel ceramic functions as a universal radiation shield, the present study evaluates its effectiveness against reactor neutrons. Since neutrons induce activation and secondary γ-ray emission in materials, we examined not only the shielding capacity but also these associated phenomena. The findings of this study may broaden the selection of shielding materials for nuclear reactors and accelerator facilities where neutron generation is expected.

EXPERIMENTS: In the current fiscal year, additional experiments were conducted to enhance the reliability of the data by expanding the experimental dataset. While the methodology follows our previous report [3], a summary is provided below. The neutron shielding effectiveness was evaluated using the transport system at the Heavy Water Neutron Irradiation Facility (HWNIF). For this evaluation, three types of samples—ceramics, lead (Pb), and iron (Fe)—were prepared with dimensions of 10 cm × 10 cm and a thickness of 1 cm, and were utilized in a stacked configuration. The activation characteristics were assessed using the rail system at the HWNIF. For this purpose, samples of the same materials were fabricated with dimensions of 2 cm × 2 cm × 1 cm. These samples were subjected to neutron irradiation for periods of 5 and 50 minutes, and their induced activation was analyzed using a High-Purity Germanium (HPGe) semiconductor detector. Furthermore, prompt γ-ray analysis was performed using the Prompt Gamma-ray Analysis (PGA) system installed at the neutron guide tube (E-3). Samples of the same size as those in the previous experiment were irradiated at 1 MW for a duration of 5 hours.

RESULTS: The experiments conducted in the current fiscal year followed the same procedures as those of the previous year to enhance data reliability, and the results obtained were largely consistent (data not shown) [3]. Specifically, the shielding capacity of the investigated ceramics against total radiation followed the order of Fe > Ceramics > Pb. For thermal neutrons, the shielding capacity was observed to be Fe > Ceramics ≈ Pb. Regarding activation characteristics, the induced activity ratio followed the order of Fe > Ceramics > Pb. Furthermore, in terms of prompt γ-ray emission, the results indicated a trend of Fe ≈ Ceramics > Pb. These findings suggest that while the novel ceramics demonstrate a certain degree of neutron shielding capability, there remain challenges concerning material activation and prompt γ-ray emission.

REFERENCES:

[1] Environmental Health Criteria 85, Lead—Environmental Aspects, World Health Organization (1989)
[2] M. Isobe *et al*., Radiat. Safety Management, **22** (2023) 1-6.
[3] H. Terato, Y Sakurai, KURNS Progress Report, **126** (2025) 126.

CO12-13

Study of neutron imaging system for ensuring safety in debris removal

N. Matsubayashi [1], T. Torii [2], S. Kurosawa [3], and M. Sasaki[4]

[1] *Institute for Integrated Radiation and Nuclear Science, Kyoto University*
[2] *Institute of Environmental Radioactivity Measurements and Forecasting Division, Monitoring Systems Development, Fukushima University*
[3] *Graduate School of Engineering, Tokyo University*
[4] *Japan Atomic Energy Agency*

INTRODUCTION: In the debris removal for decommissioning of 1F (Fukushima Daiichi Nuclear Power Plant), the shape of debris and surrounding environment may be changed, and neutrons may be generated. Since the debris are assumed to be unevenly distributed, an omnidirectional detector that can identify the direction of incident neutrons is required. In this study, we developed a neutron imaging system based on the omnidirectional detectors for β/γ-rays [1]. In this study, irradiation tests were conducted in Kyoto University Research Reactor (KUR) to evaluate the performance of the imaging system.

EXPERIMENTS: The developing omnidirectional detector is based on the FRIE (Fractal Radiation Imaging Elements) detector, a radiation imager for β/γ-ray measurement with a Sierpinski tetrahedron shape [1]. The FRIE for neutron (nFRIE) combines neutron scintillators and shielding materials. The detector elements consist of tetrahedral acrylics and thin LiF:ZnS scintillators, and the 16 elements are installed in the fractal structure with B_4C compounds. The irradiation tests were conducted at various locations around the KUR to evaluate the direction of the neutrons and the average count rate of all elements.

RESULTS: Fig. 1 shows the photograph of the irradiation tests at the KUR. The imaging measurements were performed by rotating the detector in 30-degree increments at various positions surrounding the reactor, and high signals were obtained in the direction of the reactor at all positions. The average count rates of the 16 elements and the dose rate obtained using a neutron survey meter agreed with a deviation of 10.5%, indicating that developed detector can measure the neutron dose. In conclusion, we found that the detector we developed accurately points toward the neutron source and correlated well with the neutron dose rate.

REFERENCES:

[1] Torii. T *et al.,* Development of an omnidirectional detector., IEEE Xplore, 2023.

Fig. 1. Photograph of the irradiation test at KUR

CO12-14

Characterization of the KURNS-LINAC Neutron Source based on Indirect High-Energy Neutron Imaging

T. Kamiyama [1], R. Uemoto[2], H. Uno[2], K. Nittoh[3], M. Uematsu[3], K. Nakayama[1], J. Hori[4], K. Terada[4] and Y. Yamaguchi[1]

[1] *Hokkaido Univ.*
[2] *SHI-ATEX Co. Ltd.*
[3] *Toshiba Technical Services International Corp.*
[4] *Institute for Integrated Radiation and Nuclear Science, Kyoto University*

INTRODUCTION: We have been developing a portable neutron source evaluation method using activation foil transfer to X-ray IP film. By utilizing threshold reactions in various metal converters, it images specific energy bands. This simple, rapid, and inexpensive method is applicable to both reactors and accelerators, assessing spatial and spectral characteristics without transporting radioactive materials. In this study, we measured the secondary particle emission profile from a photonuclear reaction source system at KURNS-LINAC, an electron accelerator neutron source at the Institute for Integrated Radiation and Nuclear Science, Kyoto University. The measured secondary particle emission profile from the target system in its actual operational state was evaluated by comparing it with previously measured profiles from a same kind but standalone target at the Hokkaido University neutron source (HUNS).

EXPERIMENTS: Multiple metal activation foils for neutron recording were placed at appropriate positions near the KURNS-LINAC neutron source. After two-hour irradiation with generated neutrons and secondary particles, the beta-rays emitted from the radionuclides within the activated foils were transferred to the X-ray imaging plates (IP). This allowed for the evaluation of the spatial distribution and intensity of the generated secondary particles by neutron irradiation. We used IP readers brought from Hokkaido University and, in part, SHI-ATEX equipment at Ehime. The residual activated foils were checked for product nuclides by KURRI HPGe detector.

RESULTS: Fig. 1 shows the IP transferred image from a 200 x 300 mm^2 Al activation foil positioned to surround the KURNS-LINAC neutron source system. This is the first time that a spatial distribution image of neutrons generated by an accelerator-based system has been observed on such a large dimension. It is clearly observed that the gradation of the image corresponds to the presence of the source cooling system, and neutrons are intensely generated along the downstream direction of the incident electron beam. In KURNS-LINAC and HUNS facilities both based on electron accelerators, neutron production relies on (γ,n) photonuclear reactions driven by bremsstrahlung radiation generated within Ta (KURNS-LINAC) or W + Pb (HUNS) targets. This reaction is isotropic with respect to direction. Meanwhile, considering the strong neutron peak along downstream of the electron beam makes it essential to account for direct process nuclear reactions. This process evaluations using Zn activation foils checked by HPGe detector indicated that the X-ray beam and consequent neutrons spread at an angle of approximately 7 degrees along the electron beam downstream direction, which is consistent with the results obtained at HUNS. These findings suggest that the forward directionality of the generated neutrons basically corresponds well to that of the X-rays.

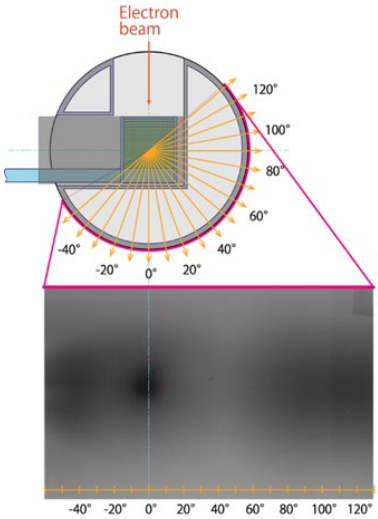

Fig. 1. Placement of a large Al activation foil (upper) and the resulting transfer image